University of Huddersfield

## University of Huddersfield Repository

Potdar, Akshay Anand, Fletcher, Simon and Longstaff, Andrew P.

Performance characterisation of a new photo-microsensor based sensing head for displacement measurement

### Original Citation

Potdar, Akshay Anand, Fletcher, Simon and Longstaff, Andrew P. (2016) Performance characterisation of a new photo-microsensor based sensing head for displacement measurement. Sensors and Actuators A: Physical, 238. pp. 60-70. ISSN 09244247

This version is available at http://eprints.hud.ac.uk/id/eprint/26740/

The University Repository is a digital collection of the research output of the University, available on Open Access. Copyright and Moral Rights for the items on this site are retained by the individual author and/or other copyright owners. Users may access full items free of charge; copies of full text items generally can be reproduced, displayed or performed and given to third parties in any format or medium for personal research or study, educational or not-for-profit purposes without prior permission or charge, provided:

- The authors, title and full bibliographic details is credited in any copy;
- A hyperlink and/or URL is included for the original metadata page; and
- The content is not changed in any way.

For more information, including our policy and submission procedure, please contact the Repository Team at: E.mailbox@hud.ac.uk.

http://eprints.hud.ac.uk/

Sensors and Actuators A 238 (2016) 60–70

Contents lists available at ScienceDirect

Sensors and Actuators A: Physical

journal homepage: www.elsevier.com/locate/sna

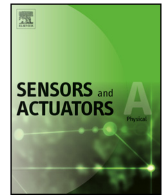

# Performance characterisation of a new photo-microsensor based sensing head for displacement measurement

Akshay Anand Potdar*, Simon Fletcher, Andrew P. Longstaff

*Centre for Precision Technologies, School of Computing and Engineering, University of Huddersfield, Queensgate, Huddersfield HD1 3DH, UK*

ARTICLE INFO

*Article history:*
Received 2 September 2015
Received in revised form 2 December 2015
Accepted 6 December 2015
Available online 11 December 2015

*Keywords:*
Displacement sensor
Nanometer-scale resolution
Micrometer range
IR slotted photomicro-sensors (SPMs)
Mechanical shutter
Self-correction arrangement

ABSTRACT

This paper presents a robust displacement sensor with nanometre-scale resolution over a micrometre range. It is composed of low cost commercially available slotted photo-microsensors (SPMs). The displacement sensor is designed with a particular arrangement of a compact array of SPMs with specially designed shutter assembly and signal processing to significantly reduce sensitivity to ambient light, input voltage variation, circuit electronics drift, etc. The sensor principle and the characterisation results are described in this paper. The proposed prototype sensor has a linear measurement range of 20 μm and resolution of 21 nm. This kind of sensor has several potential applications, including mechanical structural deformation monitoring system.

© 2015 The Authors. Published by Elsevier B.V. This is an open access article under the CC BY license (http://creativecommons.org/licenses/by/4.0/).

## 1. Introduction

Displacement is one of the fundamental variables which are required to be measured, indicated, transmitted or controlled in many industries or scientific fields for various applications. Displacement sensors can therefore be used to detect a range of measurands such as deformation, distortion, thermal expansion, vibration, strain, mechanical shock and many more [1–3]. Several physical properties are utilised in different types of displacement transducers [4,5]. Some of the commonly commercially available sensors are based upon capacitance [6], induction, eddy current [7], linear variable differential transformers (LVDT) [8], optical interferometry [9], optical linear encoders [10], laser triangulation [11], confocal principle [12], etc. Often the measuring range, resolution, bandwidth, etc. can vary significantly even for sensors utilising the same physical properties either due to the sensor design or the signal conditioning. It is therefore difficult to give precise general descriptions of their capabilities as a generalisation. However some example values can be provided based on a review of specification sheets and values in the review article by Fleming [13].

### 1.1. Review of commonly used technologies

Capacitive sensors have a typical measurement range of 10 μm–10 mm with a resolution in the order of 1 nm. Eddy current sensors typically have a linear range of 100 μm–80 mm and resolution in the order of 10 nm. Interferometers (excluding those designed for short range surface measurement) can operate over several metres and typically have a resolution of 1 nm. LVDT's usually operate over 0.5–500 mm with resolution of 5 nm [13]. Optical sensors based on the laser triangulation principle generally have measuring range of few millimetres and a resolution of 0.005% of Full Scale Output (FSO) [14]. Laser confocal sensors have a typical measurement range of 0.3–30 mm with resolution of 0.004% of FSO [15].

Capacitive sensors are relatively simple in construction and provide the highest resolution over short ranges. However, they are sensitive to the surface irregularities, variations in humidity and temperature. Also their performance is affected by the contamination of interfacial fluid (air in most cases) which is important in industrial environments where clean measuring surfaces and environments cannot be guaranteed [16]. Eddy current sensors are insensitive to dirt, dust, oil and moisture/coolant and can be used with all electrically conductive materials [17] but are more sensitive to temperature than capacitive sensors [18]. Inductive sensors have been also developed, but nanometric resolution remains

* Corresponding author.
*E-mail addresses:* akshay.potdar@hud.ac.uk, akshay01@gmail.com (A.A. Potdar).

http://dx.doi.org/10.1016/j.sna.2015.12.007
0924-4247/© 2015 The Authors. Published by Elsevier B.V. This is an open access article under the CC BY license (http://creativecommons.org/licenses/by/4.0/).

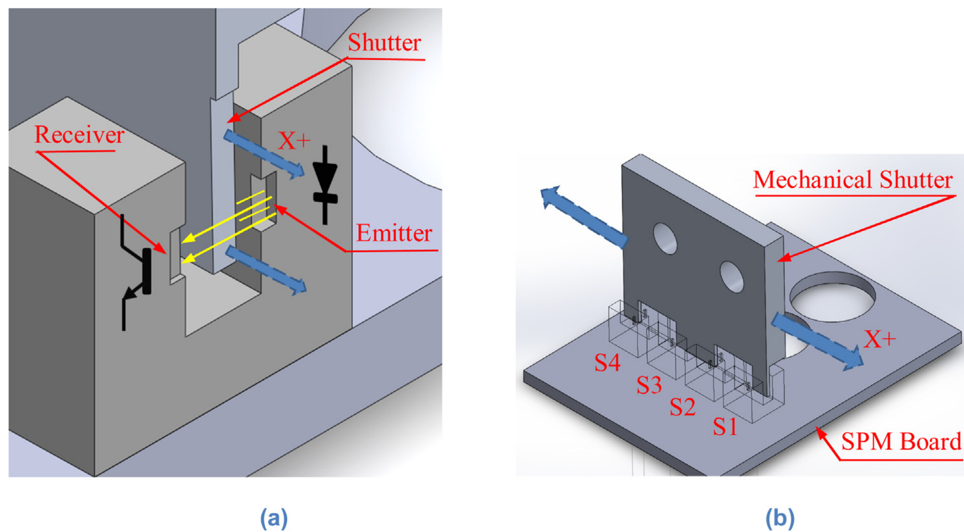


**Fig. 1.** (a) Cross section view of a single sensor and shutter and (b) schematic of the overall system.

difficult to reach because of magnetic disturbances and variability in the subsurface material causing electrical run-out. LVDT sensors are amongst the most popular in industrial applications. They are simple and hence robust, have a high intrinsic linearity and can be magnetically shielded. However their maximum resolution is limited by the physical construction of the transducer which is generally suited to ranges greater than 1 mm [13].

Compared to other sensor technologies, laser interferometers and optical linear encoders provide a good solution in terms of nanometre resolution over longer distances such as a few metres of range. Nevertheless their price, complexity of installation, alignment and relatively large space requirement for operation can be prohibitive in many applications [19]. The triangulation based optical displacement sensor operation is dependent upon the surface texture (energy reflectance characteristics of surfaces being examined) of the target [20] and the sensor head is relatively large compared to other systems due to the integrated electronics and optical detector. They have also been found to have significant issues of self-heating, requiring periods of tens of minutes to achieve thermal equilibrium. The laser confocal sensor requires a clean environment in the optical path for accurate operation.

Sensors are also fundamental in closed loop control systems. The capability to develop integrated and compact apparatus is still a key point for most measurement and control systems [21]. It is therefore imperative that they are robust to self-induced or unwanted exogenous influences.

Optical sensors are particularly useful in a number of applications since they are often relatively immune to various perturbations like stray electromagnetic effect, capacitive effect, etc., which are observed in many non-optical sensors [15,22]. However, such systems can be affected by thermal distortion (misalignment of optical receivers) [3] or contamination by ambient light [23]. They must therefore be fully evaluated before being applied to measurement or control problems. Fibre bragg grating (FBG) displacement sensors are receiving more attention owing to all the inherent advantages of optical fibre [24] and due to the advantages such as wavelength encoded information, they offer immunity against source power fluctuations as well as insusceptible to noise caused by variations in light levels [25]. However, cost of interrogation systems for FBG sensors is very high. In addition, temperature compensation is required for pure displacement measurement applications, increasing complexity of the system [26].

### 1.2. *Research into low cost solution*

A significant amount of research has been carried out to develop sensors or measurement systems combining the advantages of simplicity, high resolution and low price. Low-level technological barriers can be rapidly addressed by making adapted use of mass-produced components for consumer electronics. Due to the various advantages discussed above, low cost optical sensors have been investigated for use for displacement measurement. For example, Delmas [27] proposed a system where the displacement of a moving stem is measured by an optoelectronic displacement measuring sensor consisting of a light source (Light Emitting Diode) and light sensitive sensor (Photodiode). A similar optoelectronic displacement sensor has been designed for the absolute measurement of displacement in the micrometre range [28].

Shan et al. [29] evaluated the performance of a low cost reflective IR (focussed and non-focussed) sensor for measurement of a $\pm 200\,\mu m$ range and found that its performance (focussed) was comparable with commercially available inductive sensor in terms of linear distortion, range and bandwidth. The unfiltered resolution of the IR sensor was within sub-microlevel range but the specific value was not quoted. The observed maximum sensitivity was $0.010\,V/\mu m$ and $0.002\,V/\mu m$ for non-focussed and focussed IR sensors, respectively. This type of sensor requires sufficiently large reflective target size (at least twice the lens surface area for focussed sensor and six times for non-focussed). Performance of the reflective sensor based on the intensity of the back scattered IR light is dependent on the reflectance of the surrounding object and can produce imprecise results [30] and requires more complex techniques such as phase shift measurement and triangulation for range measurement. Lin et al. [23] used a single transmissive IR photo-interrupter (with collimated lenses in front of source and collector) with knife edge to develop a displacement sensor with a range greater than $100\,\mu m$ and the experimentally obtained maximum sensitivity was $0.2\,V/\mu m$. To lower the effect of the thermal expansion of the steel knife-edge, another block of aluminium coated silica was prepared, but the experimental results of use of this new block were not mentioned.

The effects of ambient light variation have not been considered in the evaluation of Shan et al. [29], or Lin et al. [23], where the entire setup was covered in opaque box with external lights turned off. In an industrial environment, variation in ambient light conditions is inevitable unless uninterrupted guarding is present, so it is necessary to study its impact on the output of the sensor. Neither paper

reported the effects of environmental temperature fluctuations or the long-term stability of the sensor.

This paper describes the development and characterisation of a new displacement sensor head, which utilises commercially available and inexpensive (USD 0.71 each) infrared (IR) transmissive sensors, also known as slotted photo-microsensors (SPMs) or photo-interrupters. The design of a prototype nanometre-scale resolution displacement sensor, based on an opto-electro-mechanical sensing head is described. The proposed sensor head has been designed to significantly reduce influence of ambient light, input voltage variation and sensor electronics drift. Experiments for characterisation of the proposed sensor were performed and experimental results have been stated in the paper. A linear measurement range of 20 μm has been observed for the prototype SPM head, over which the repeatability was measured as 90 nm and resolution of 21 nm.

## 2. Principle of measurement

The principle of measurement for the new displacement sensing head is based upon optoelectronic sensing of the position of the specially designed moving mechanical shutter. Fig. 1a illustrates the principle of operation of the sensors. Each sensor is composed of an infrared emitter (light emitting diode) on one side and an infrared detector (phototransistor) on the other side facing each other, separated by a small gap in which the mechanical shutter is situated. The movement of the shutter is proportional to the displacement encountered by it, resulting in a change in the amount of obstruction to the optical path between the emitter and receiver. Since the output voltage from the receiver is a function of the intensity of light beam incident on it, the corresponding movement of the shutter will be detected. The sensing range depends upon the gap between emitter and receiver.

It was observed during the benchmark testing that the single sensor output voltage is sensitive to the supply voltage variations, ambient light and temperature changes; this is to be expected given that the sensors are typically used for binary presence detection in process control applications and such small drifts would not be an issue. To improve the stability of the sensor, the head design incorporates four SPMs, S1–S4, acting together with a specially designed shutter (Fig. 1b) to provide cancellation. The shutter is designed to cluster the sensors pairwise; it blocks the light to one sensor while simultaneously allowing the light on the second sensor. Thus, sensor S1 and S2 form a pair; when S1 loses the light, S2 gains the light in same proportion. Similarly, S3 and S4 form another pair. This produces a differential voltage output for each pair, cancelling the effect of input voltage variation. Averaging the two differential outputs reduces the influence of ambient light variations and differential thermally induced expansion between the sensor circuit and shutter. This novel arrangement allows self-correction for the external perturbations as mentioned earlier. Eq. (1) represents the displacement of the shutter with output voltages of all the sensors.

$$D = K \times \frac{\left[\frac{(V1-V2)}{2} + \frac{(V3-V4)}{2}\right]}{2} \quad (1)$$

where $D$ is the displacement (μm), $K$ is a calibration constant (μm/mV), $V1$–$V4$ are the output voltages of SPM1–SPM4 ($V$).

## 3. Prototype system

The design of the proposed prototype opto-electro-mechanical head assembly is shown in Fig. 2. The shutter is mounted on the shutter head and the SPM board, which will then be attached to an amplification device, while the SPM board is mounted on the reference structure. There are vast array of different SPM sensors available in the market. The type used in the prototype device was selected on the basis of its low cost, compact size (3.4 mm × 3 mm × 3 mm) and small aperture width of 150 μm for high sensitivity. Additionally, the chosen unit has a gap between emitter and receiver of 1 mm, which is sufficiently small that it reduces the effect of incident ambient light variation with free movement of the shutter; this ensures optimum light transfer. The realisation and physical dimensions of the SPM board are represented in Fig. 3.

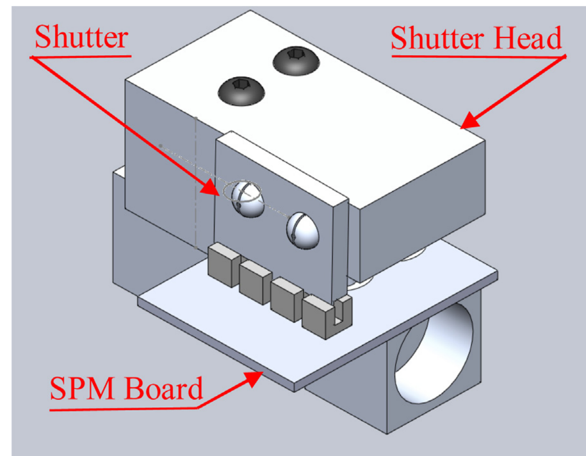


**Fig. 2.** Sensing head.

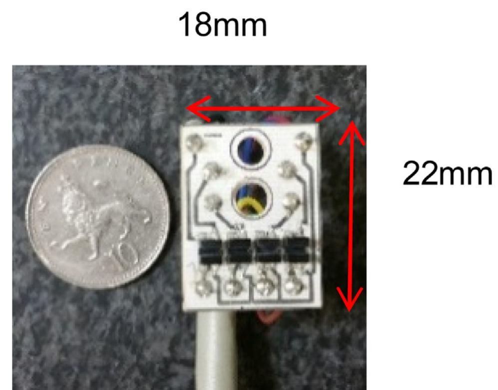


**Fig. 3.** Prototype SPM board.

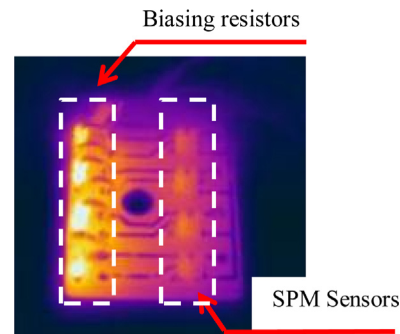


**Fig. 4.** Thermal image of the biasing resistors.

The biasing circuit used to establish proper operating conditions for the SPMs, is designed to be remote from the SPM board in order to avoid the effect of local self-heating from electrical components. Fig. 4 shows a thermal image of the first design of the SPM board, highlighting the heat input from the biasing resistors where the SPMs and their corresponding biasing resistors were on the same

board. It can be seen that temperature of the resistors is significantly higher than the SPMs. In order to minimise the cost of the overall setup, standard resistors (330 Ω, 1/2 W) were used.

The mechanical shutter, shutter head and sensor base were manufactured using aluminium to reduce the thermally induced errors in the sensor. Although aluminium has a high coefficient of thermal expansion, using the same material throughout, coupled with the high thermal conductivity, means that the head assembly and self-correction mechanism of the setup will be more reliable than using more exotic materials, for the given cost.

A Farnell L30-2 stabilized power supply is used to provide power to the entire electric circuit. Raw output voltages generated by the sensing head proportional to the displacement are fed into the analogue to digital converter (ADC: NI-USB 6363, 16-bit resolution). This ADC output is then further given to the data logging computer. An in-house developed LabVIEW program [31] is used to convert the voltages into the equivalent displacement using Eq. (1).

## 4. Sensor characterization

A schematic of the experimental setup used to perform a series of tests on the sensing head for characterisation is shown in Fig. 5. Fig. 6 shows a photograph of the actual setup. The equipment was placed on the granite bed of a Coordinate Measuring Machine (CMM) (Zeiss Prismo Access 09/18/09) as a mechanically and thermally stable reference. In particular, the SPM board was located on the granite bed and the shutter head was mounted on the head of the CMM. The CMM was located in a temperature controlled room which was measured to be 21 °C ± 1 °C, during the entire duration of the tests, with the exception of tests requiring specific temperature variation for thermal characterisation. For the purpose of this test, the CMM axes were used to produce the required displacement. This was convenient and provided good control for small movements.

Tests were performed by moving the CMM over the entire range of the sensor head in increments of 2 μm. A Renishaw XL-80 laser Interferometer system (accuracy: ±0.5 ppm, resolution: 1 nm and range 80 m) was used as the independent reference measurement of the displacement. Retro-reflector optics of the laser were attached to the bottom of the CMM head and the shutter of the sensor was fixed to the one end of the retro reflector (Fig. 7). Thus, the shutter of the SPM head and the laser's optics experiences the same displacement. Test results are discussed in the subsequent sections.

### 4.1. Characteristic curve

The experimentally obtained static characteristic curve of the sensor is shown in Fig. 8, illustrating the variation in SPM head output voltages with change in shutter position measured by the XL-80 laser interferometer. It can be observed that the relationship between measured voltage and displacement is non-linear in nature and the sensitivity (gradient) of the curve is not consistent over the entire input displacement range.

The characteristic curve was divided into three sections based upon the change in the slope by finding the first derivative; the two end sections (1 and 3) have non-linear response and a middle section (2) where the output is proportional to the input. The slope of section 2 was found to be 0.17 V/μm. This characteristic allows the sensor to be used reliably over the given input range with a well-determined output. Sections 1 and 3 could also be used with further refinement, but for the remainder of this work, only the linear portion is investigated.

**Table 1**
The Standard deviation (SD) at each position.

| Displacement (μm) | 0 | 2 | 4 | 6 | 8 | 10 | 12 | 14 | 16 | 18 | 20 |
|---|---|---|---|---|---|---|---|---|---|---|---|
| Forward SD (nm) | 0 | 47 | 60 | 33 | 28 | 31 | 41 | 35 | 50 | 42 | 60 |
| Reverse SD (nm) | 21 | 35 | 62 | 35 | 71 | 25 | 73 | 77 | 48 | 86 | 60 |

### 4.2. Calibration of the characteristic curve and linear range of the sensor

Calibration of the curve is performed using the Least Square Regression (LSR) technique. The linearly fit curve is specified by Eq. (2).

$$V = sD + d_o \quad (2)$$

where $V$ is the SPM output voltage ($V$), $s$ is the sensitivity (V/μm), $D$ is the displacement (μm) and $d_o$ is an offset.

The mean value of the sensitivity obtained by LSR is 0.1648 V/μm with confidence interval of ±0.0009 for 99% confidence level using Student's $t$-distribution. For all further calculations, this value will be used over the full scale range (FSR) of 20 μm.

Since the linearisation function described by Eq. (2) is an approximation of the actual curve, it does not describe the actual curve perfectly introducing the mapping linearity error. Fig. 9 shows the mapping linearity error in terms of percentage of FSR after least square fitting was removed. It is calculated using Eqs. (3) and (4).

$$e_m(v) = f_a(v) - f_{cal}(v) \quad (3)$$

where, $e_m(v)$ is a mapping error in volts, $f_a(v)$ is an actual output obtained by experiment and $f_{cal}(v)$ is the predicted value obtained by calibration curve. The value of $e_m(v)$ is then converted into microns using the value of sensitivity achieved from Eq. (2).

$$\text{mapping error}\,(\%) = \pm \frac{\max|e_m|}{\text{FSR}} \times 100 \quad (4)$$

where, $\max|e_m|$ is a maximum mapping error, which is within ±0.2 μm. Thus, the linearity error due to the calibration curve approximation is found to be within ±1% of FSR.

### 4.3. Repeatability

In order to find the sensor repeatability, the same test was repeated five times over the entire linear range under the same operating conditions. The output value of the SPM head and corresponding XL-80 laser interferometer reading was recorded for targets every 2 μm of CMM displacement in a bi-directional test. Fig. 10 illustrates the deviation in SPM measurement readings from the laser for the five tests. The standard deviation (SD) at every target position was calculated and the maximum SD among all the positions in both the directions was considered as the repeatability of the sensor; the ISO 5725 defines the repeatability as the precision (one SD) under repeatability condition [32]. Table 1 shows the SD of all positions in the forward and reverse direction. Thus, the proposed sensor has a repeatability of 90 nm.

### 4.4. Resolution and noise

The resolution of sensors is often limited by the noise in the overall measurement system rather than the ADC resolution (which in this case is 1 nm using 16-bit ADC for 0.1648 V/μm of sensitivity). An uncertainty is introduced in the measured displacement value due to random noise. This uncertainty can produce an error in the sensor output if the measured readings are closer to each other than the value of the uncertainty. The resolution can be quantified then

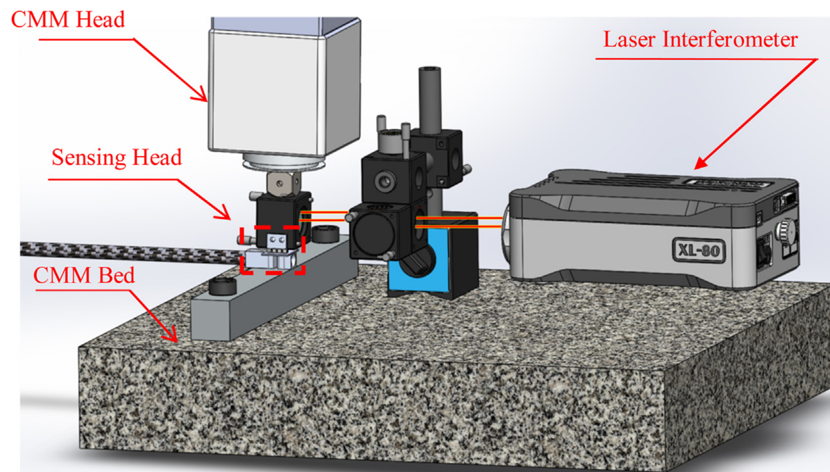


**Fig. 5.** Schematic of sensor calibration setup.

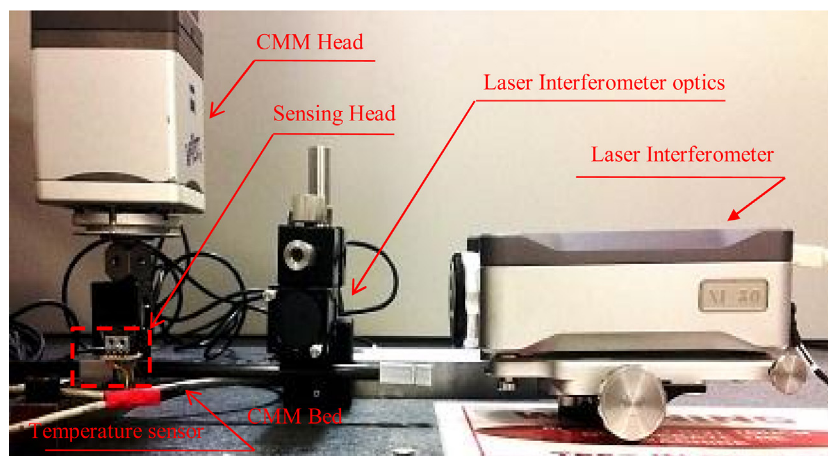


**Fig. 6.** Sensor calibration setup.

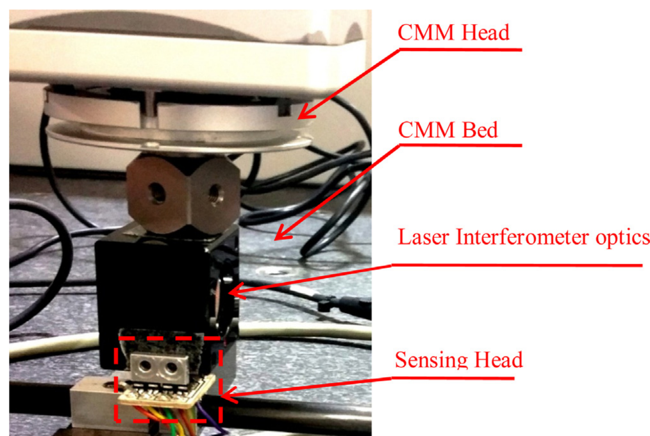


**Fig. 7.** Close up of CMM and SPM sensor head setup.

by a multiple of the standard deviation (σ) of the noise. The noise level is calculated to be 6σ to achieve 99.7% confidence [13].

The sensor was quantified for static performance at ten places along its measurement range. The data was captured at 1 kHz and the corresponding standard deviations were calculated. The worst case, at one of the extremities, is presented in Fig. 11. This therefore shows a worst-case noise floor of 6σ = 21 nm across the sensor's measurement range, when used statically.

To validate the resolution of the sensor in dynamic operation, a small PZT (Lead Zirconate Titanate) actuator P-810.10 from Physik Instrumente (PI) GmbH was utilised to generate very small movements. The PZT was directly attached to the rear end of the XL-80 retro reflector. The resolution of the sensor head was determined by applying a sinusoidal signal with varying amplitude from a function generator to PZT actuator. The amplitude of the signal was reduced in each cycle until the SPM head was unable to detect

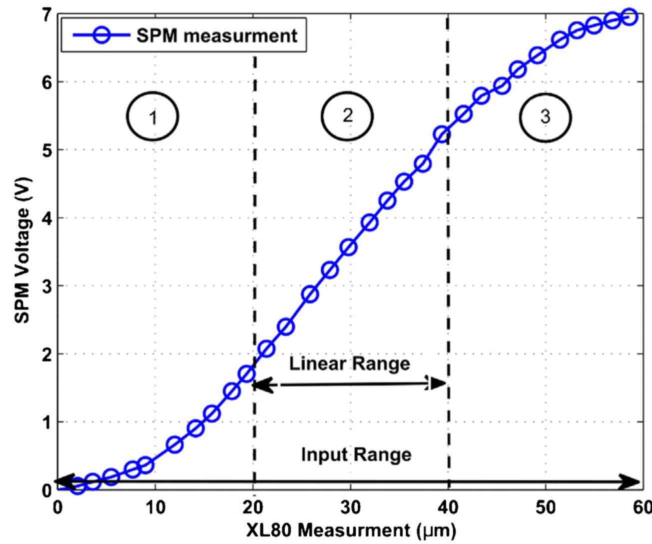


**Fig. 8.** Characteristic curve of SPM head.

the sinusoidal wave. The PZT was excited by a sinusoidal signal of 1 Hz frequency with amplitude of 0.6 V and corresponding readings were measured.

Fig. 12a illustrates the SPM head output with low pass filter at 10 Hz. Fig. 12b shows the measured voltage equivalent displacement of the SPM head and the output of the XL-80 laser interferometer. As it can be observed, the SPM output is sinusoidal in nature and is comparable with the reference measurement from the laser. A short time delay can be noticed between the two signals, this is due to the mismatch between trigger inputs of the two data logging applications. Due to the very small magnitude of the sinusoid, the SPM head result includes the SPM noise and mechanical noise in the setup; both SPM head and XL-80 measurement are affected by noise in the setup equally and hence can be ignored. The SD of noise in SPM head is 17 nm and that of XL-80 is 13 nm. Thus, system resolution is comparable to that of laser interferometer.

### *4.5. Immunity against variation in power supply and ambient light*

Stability of the SPM head output depends on the stability of the input power supply. Any variation in the power supply will affect the intensity of the light beam emitted by the LED. This in turn will have an effect on the incident light on a receiver. Since displacement is a function of the intensity of an incident light on the receiver, there is a possibility of a false displacement reading with respect to input voltage.

Thus, a stabilised DC power supply was used to energize the circuit. However, in the field it is possible that output of the DC power supply is susceptible to variation in mains-line power. In order to reduce the effect of power supply variation, as mentioned in Section 2, a four-sensor configuration was used to design the SPM sensor and Eq. (1) was used to calculate the final output.

To investigate the sensitivity of a sensor to power supply variation, the output of the DC supply voltage was changed within ±10 mV and the output of all four sensors S1, S2, S3 and S4 was measured as *V*1, *V*2, *V*3 and *V*4. Fig. 13 shows the (a) differential voltage (DV1) output between sensor S1 and S2, (b) differential voltage (DV2) output between sensor S3 and S4 as well as (c) average of the two differential outputs (DV1 and DV2). It can be clearly seen that from Fig. 13 that the use of the differential voltage schema reduces the influence of power supply variation and the final average output voltage of an SPM head is within ±2 mV, which equates to ±12 nm.

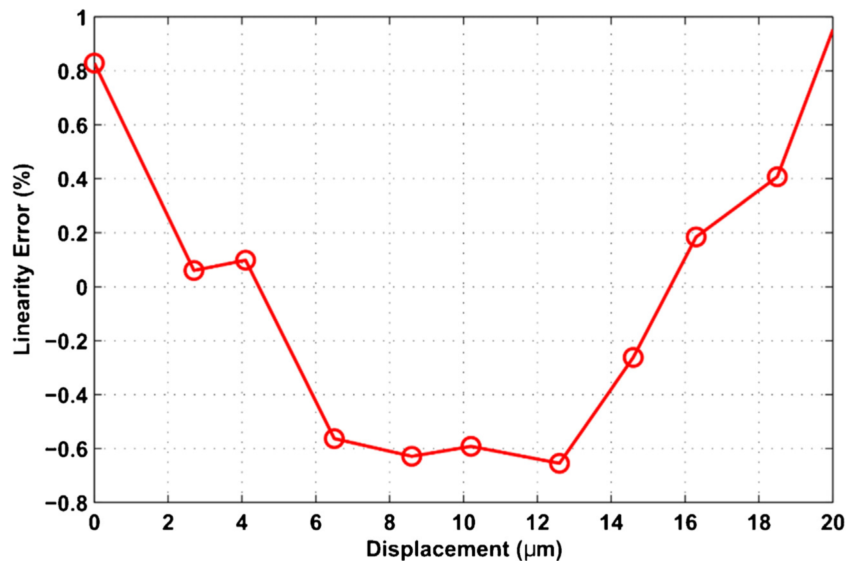


**Fig. 9.** Mapping Error due to calibration curve approximation.

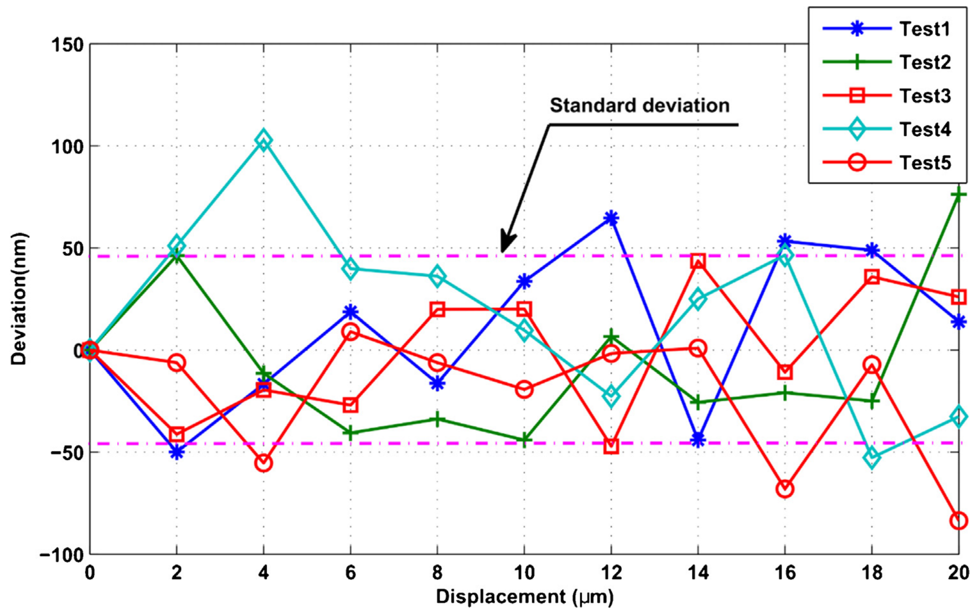


**Fig. 10.** Repeatability test for the sensor head.

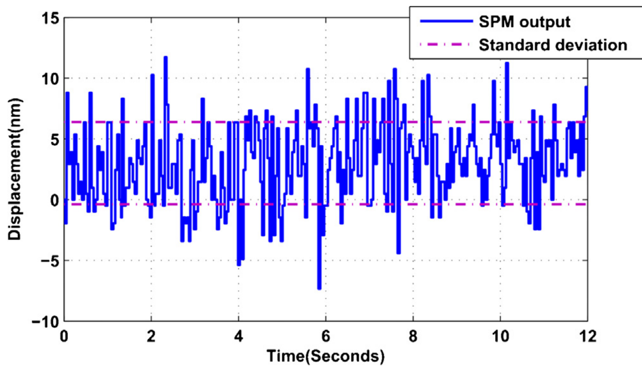


**Fig. 11.** Time domain recording of the sensor head output sampled at 1 KHz.

Change in ambient light can also cause misreading of optical systems. In the prototype head, the receiver (phototransistor) has peak spectral sensitivity wavelength of 920 nm in the spectral range of approximately 850–975 nm with 90% relative sensitivity. The emitter has peak emission wavelength of 940 nm, which is near to the peak spectral sensitivity wavelength of the receiver. The small size of the emitter and receiver aperture window (width of 150 μm) with gap of 1 mm between emitter and receiver along with meticulous sensor head design can minimise the influence of ambient light.

The four sensor configuration helps to reduce the effect of ambient light; to examine this, strobe light effect using white LED source was generated. The intensity of the light was kept at 250 and 360 Lux to simulate the factory conditions. The results of the test at 250 Lux is shown in Fig. 14. Differential voltages DV1 (Fig. 14a) and DV2 (Fig. 14b) decreases the effect variations in individual sensor outputs ($V1$, $V2$, $V3$ and $V4$) due changes in the incident light. The SPM output, which is an average of DV1 and DV2, keeps the final output within ±1 mV (±6 nm). The results at 360 Lux were identical. Further improvements in the results can be achieved by keeping the sensor inside an enclosure to protect from ambient light variations.

### 4.6. Sensor drift

Long term stability of the sensor is important, to ensure the validity of the measurement results. Drift in the displacement sensor output can take place even though there is no change in the environmental or measurement conditions, due to signal conditioning electronics for example and is normally measured against elapsed time.

This experiment was conducted in a temperature controlled environment, in which the temperature variation was maintained at less than 1 °C. The experimental setup is shown in Fig. 5. The temperature was measured using a digital temperature sensor DS18B20 and the test duration was 9 h. This test was run by keeping the mechanical shutter nominally stationary for the entire duration. The Renishaw XL-80 laser interferometer was used to validate the test results.

Fig. 15 shows the result of the conducted experiment. The measured environmental temperature variations were within 0.5 °C. The SPM head output during this period changes by 0.22 μm and the XL-80 reading changes by 0.3 μm. The deviation in the differential displacement between SPM head and XL-80 reading is within ±0.2 μm; some of the detected variations are likely due to the quantization of the XL-80 long term logging application. Thus, in a relatively stable temperature, the differential drift between the XL-80 and SPM head is less than the uncertainty of the setup.

To investigate the effect of setup temperature variation on the prototype SPM sensor head, the temperature of the environment was increased using a heating coil (2000 W) for two and half hours (Heating process) and then allowed to cool down. The heating coil temperature was gradually increased to avoid any thermal shock to the CMM structure. The results are shown in Fig. 16.

For the purpose of analysis, the differential displacement between the XL-80 and SPM head on the experiment (shown by the green line in Fig. 16) can be considered to isolate the effect of thermal distortion of a CMM structure. The XL-80 optics were carefully setup (Fig. 6) to minimise the effect of dead path error and Abbe error, which were reduced to 75 mm and 25 mm respectively. During the first 50 min of the heating cycle, initial drift of 0.8 μm can be observed in the differential displacement (shown by green line in Fig. 16); thereafter displacement variation is within 0.4 μm for rest of the heating cycle. The displacement is a

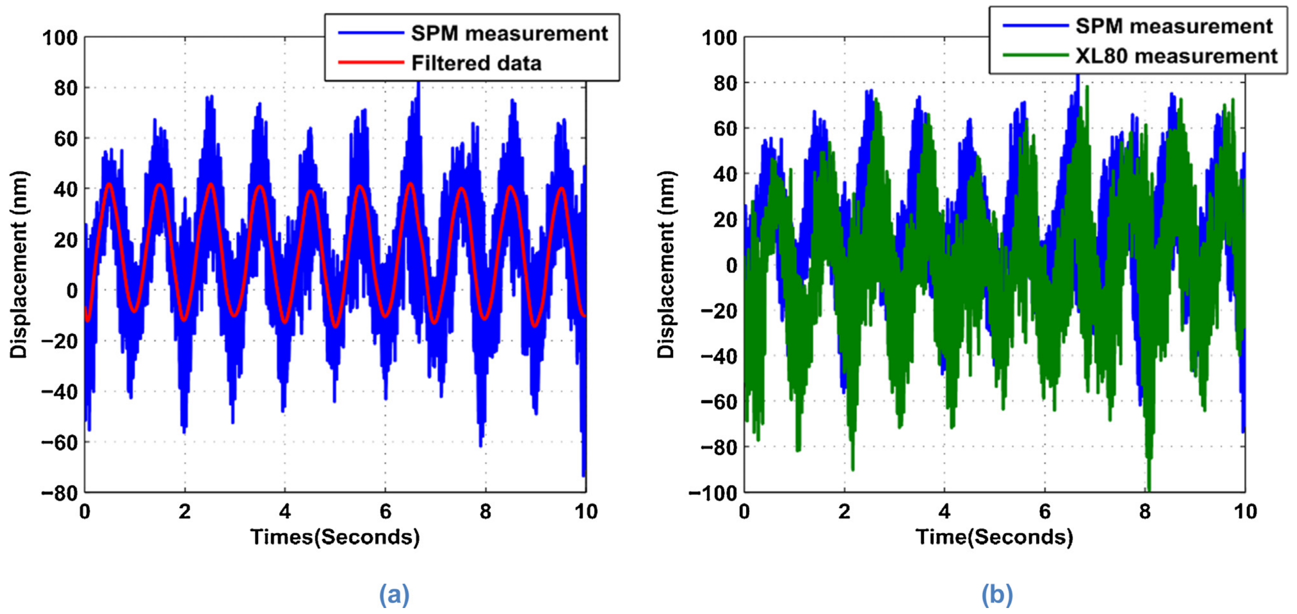


**Fig. 12.** SPM sensor head resolution test result.

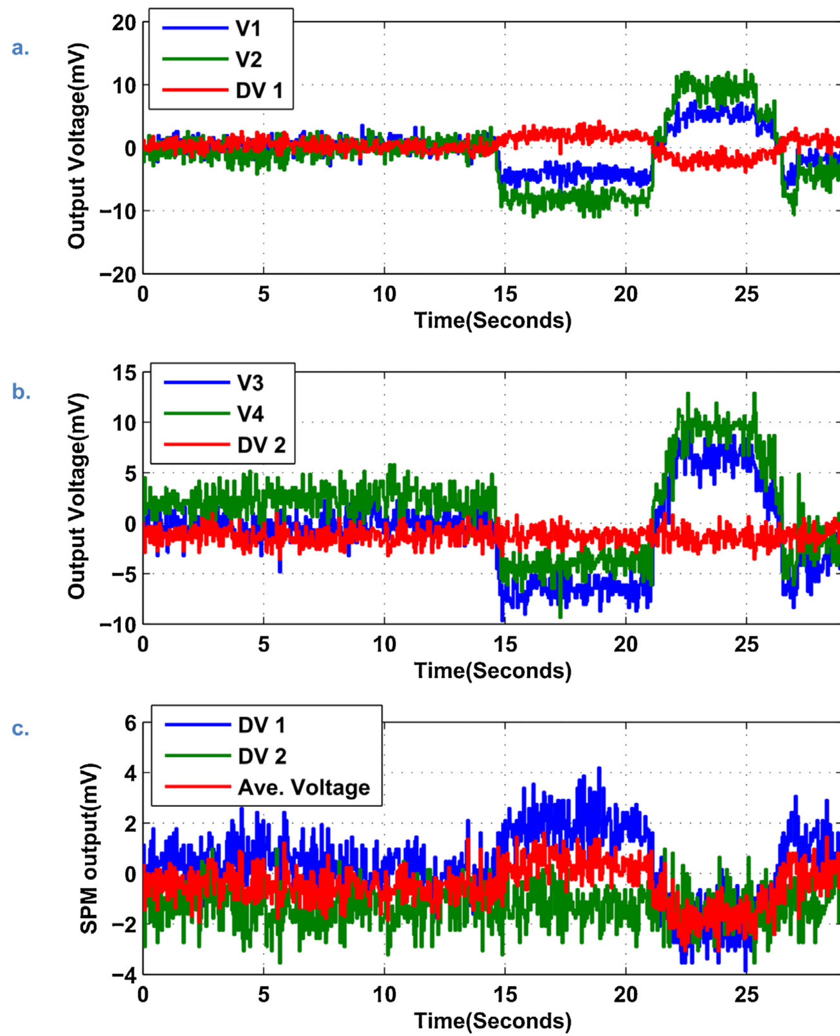


**Fig. 13.** SPM sensor head insensitivity to the variation in power supply voltage; (a) Differential voltage (DV1) between sensor S1 and S2, (b) differential voltage (DV2) between sensor S3 and S4, (c) final SPM output (average voltage).

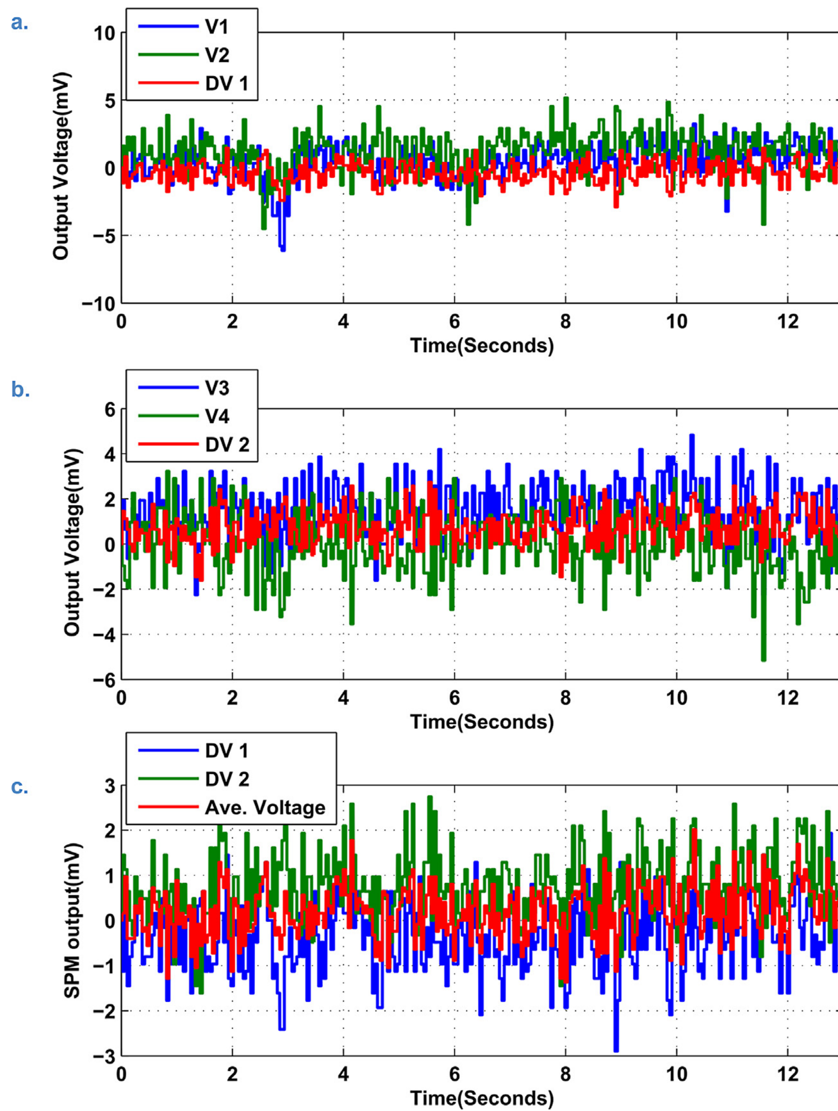


**Fig. 14.** SPM sensor head insensitivity to the variation in ambient light; (a) Differential voltage (DV1) between sensor S1 and S2, (b) differential voltage (DV2) between sensor S3 and S4, (c) final SPM output (average voltage).

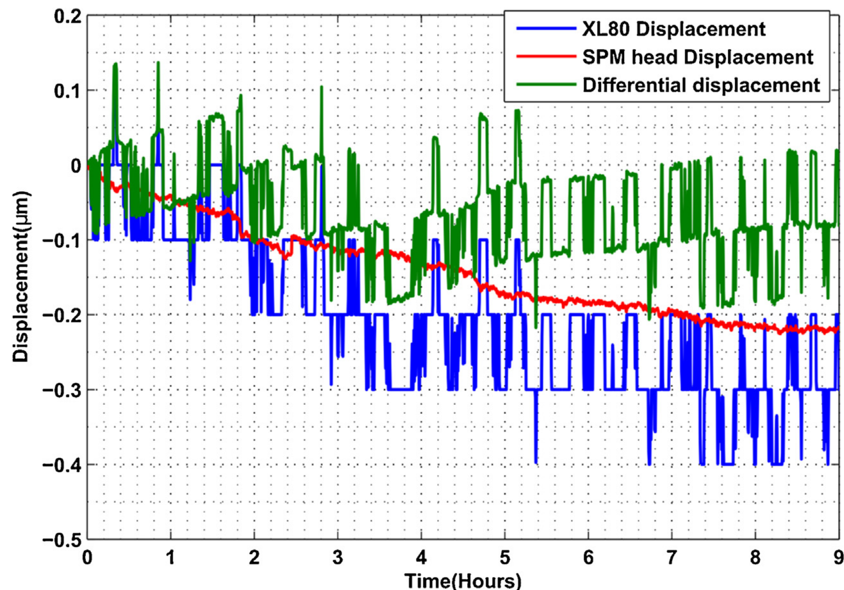


**Fig. 15.** Measurement results for SPM head stability test.

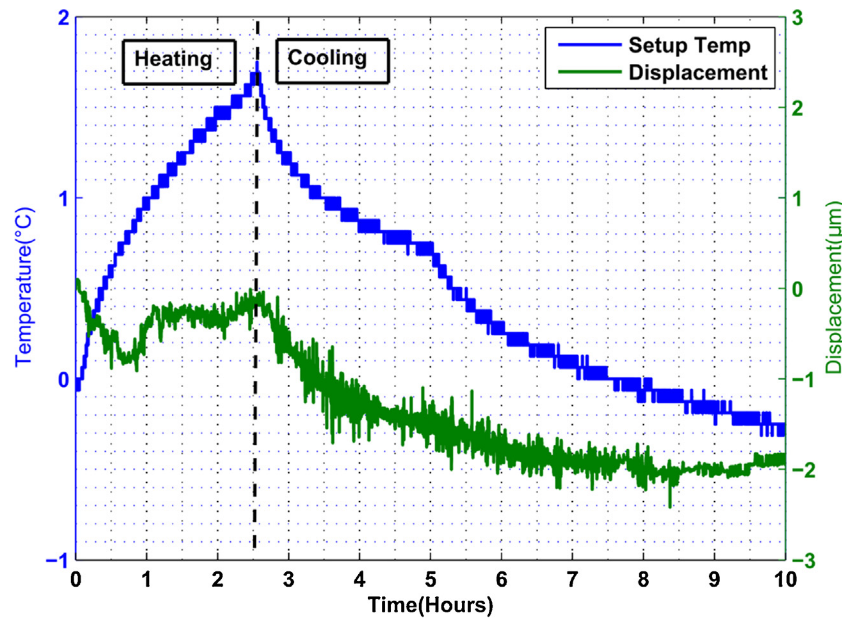


**Fig. 16.** Temperature drift of the SPM head.

maximum of 2 μm during the cooling cycle for a drop in temperature of 2 °C. It can be observed that parameters are related but there is no direct correlation of the sensor output deviation to the temperature. It is assumed that the variation is likely due to the residual offsets of the setup and CMM movement. The results confirm that the sensor is very robust to ambient temperature variation.

## 5. Conclusion

In this paper, the design of a new nanometre-scale resolution displacement sensor based on an opto-electro-mechanical sensing head has been described and the capabilities of a prototype system have been fully characterised. The proposed system is capable of self-compensation against the perturbations due to power supply and ambient light variations. Although the design of the shutter is in contact with the object to be monitored, overall sensor design is minimally invasive. The cost of the prototype sensor head is 40 USD, less than 10% of their uncalibrated capacitive and inductive counterparts without electronics. The output of the sensor is compatible with any standard data acquisition hardware and software. It is a low cost, compact sized sensor with small footprint that can be designed with a relatively small number of components without any complex signal processing circuits.

Static and dynamic experiments were carried out to investigate the performance characteristics of the prototype sensor head. The static linear range and resolution (6σ) were evaluated to be 20 μm and 21 nm respectively, with a sensitivity of 0.1648 V/μm. The linearity error is within ±1% of full-scale range. The repeatability of the sensor is 90 nm and the observed noise in the sensor signal is 21 nm without the use of any filter.

The practical limitation of the current implementation is the mechanical shutter design with tight tolerances on its physical dimensions. The potential applications include, but are not limited to, mechanical structural deformation monitoring, piezo-actuator control, vibration monitoring systems, etc.

The characterisation of the system presented in this paper forms the basis for an uncertainty evaluation of any measurement system that uses the proposed sensor head as its basis. The full uncertainty analysis must take into account the method of mounting and any amplification device used as well as the uncertainty of the sensing head.

## Acknowledgements

The authors gratefully acknowledge the UK's Engineering and Physical Sciences Research Council (EPSRC) funding of the EPSRC Centre for Innovative Manufacturing in Advanced Metrology (Grant Ref.: EP/I033424/1).

The work carried out in this paper is partially funded by the EU Project (NMP2-SL-2010-260051) "HARCO" (Hierarchical and Adaptive smaRt COmponents for precision production systems application). The authors wish to thank all the partners of the consortium.

## References

[1] Y. Peng, et al., A Cr–N thin film displacement sensor for precision positioning of a micro-stage, Sens. Actuators A: Phys. 211 (2014) 89–97.
[2] A. Maekawa, et al., Experimental validation of non-contacting measurement method using LED-optical displacement sensors for vibration stress of small-bore piping, Measurement 71 (2015) 1–10.
[3] G. Berkovic, E. Shafir, Optical methods for distance and displacement measurements, Adv. Opt. Photonics 4 (4) (2012) 441–471.
[4] D.J. Bell, et al., MEMS actuators and sensors: observations on their performance and selection for purpose, J. Micromech. Microeng. 15 (7) (2005) S153.
[5] H. Haitjema, P.H.J. Schellekens, S.F.C.L. Wetzels, Calibration of displacement sensors up to 300 μm with nanometre accuracy and direct traceability to a primary standard of length, Metrologia 37 (1) (2000) 25.
[6] H. Nouira, et al., Investigation of the influence of the main error sources on the capacitive displacement measurements with cylindrical artefacts, Precis. Eng. 37 (3) (2013) 721–737.
[7] M.R. Nabavi, S.N. Nihtianov, Design strategies for eddy-current displacement sensor systems: review and recommendations, Sens. J. IEEE 12 (12) (2012) 3346–3355.
[8] C. Lee, S.-K. Lee, Multi-degree-of-freedom motion error measurement in an ultraprecision machine using laser encoder—review, J. Mech. Sci. Technol. 27 (1) (2013) 141–152.
[9] J.-Y. Lee, et al., Optical heterodyne grating interferometry for displacement measurement with subnanometric resolution, Sens. Actuators A: Phys. 137 (1) (2007) 185–191.
[10] L. ChaBum, K. Gyu Ha, L. Sun-Kyu, Design and construction of a single unit multi-function optical encoder for a six-degree-of-freedom motion error measurement in an ultraprecision linear stage, Meas. Sci. Technol. 22 (10) (2011) 105901.
[11] Z. Zhang, et al., A new laser displacement sensor based on triangulation for gauge real-time measurement, Opt. Laser Technol. 40 (2) (2008) 252–255.
[12] P.J. Boltryk, M. Hill, J.W. McBride, Comparing laser and polychromatic confocal optical displacement sensors for the 3D measurement of cylindrical artefacts containing microscopic grooved structures, Wear 266 (5–6) (2009) 498–501.

[13] A.J. Fleming, A review of nanometer resolution position sensors: operation and performance, Sens. Actuators A: Phys. 190 (0) (2013) 106–126.
[14] L. Perret, et al., Fiber optics sensor for sub-nanometric displacement and wide bandwidth systems, Sens. Actuators A: Phys. 165 (2) (2011) 189–193.
[15] S.C. Bera, S. Chakraborty, Study of magneto-optic element as a displacement sensor, Measurement 44 (9) (2011) 1747–1752.
[16] M. Kim, et al., A new capacitive displacement sensor with high accuracy and long-range, Sens. Actuators A: Phys. 130–131 (0) (2006) 135–141.
[17] H. Wang, et al., Ultrastable eddy current displacement sensor working in harsh temperature environments with comprehensive self-temperature compensation, Sens. Actuators A: Phys. 211 (2014) 98–104.
[18] H. Wang, Ultrastable and highly sensitive eddy current displacement sensor using self-temperature compensation, Sens. Actuators A: Phys. 203 (2013) 362–368.
[19] A. Missoffe, et al., New simple optical sensor: from nanometer resolution to centimeter displacement range, Sens. Actuators A: Phys. 176 (0) (2012) 46–52.
[20] T. Mueller, E. Reithmeier, Image segmentation for laser triangulation based on Chan–Vese model, Measurement 63 (2015) 100–109.
[21] C. Lee, S.-K. Lee, J.A. Tarbutton, Positioning control effectiveness of optical knife edge displacement sensor-embedded monolithic precision stage, Sens. Actuators A: Phys. 233 (2015) 390–396.
[22] J. Shieh, et al., The selection of sensors, Prog. Mater. Sci. 46 (3–4) (2001) 461–504.
[23] F. Lin, S.T. Smith, G. Hussain, Optical fiber displacement sensor and its application to tuning fork response measurement, Precis. Eng. 36 (4) (2012) 620–628.
[24] P. Bosetti, S. Bruschi, Enhancing positioning accuracy of CNC machine tools by means of direct measurement of deformation, Int. J. Adv. Manuf. Technol. 58 (5–8) (2012) 651–662.
[25] J. Li, H. Neumann, R. Ramalingam, Design, fabrication, and testing of fiber bragg grating sensors for cryogenic long-range displacement measurement, Cryogenics 68 (2015) 36–43.
[26] M. Majumder, et al., Fibre Bragg gratings in structural health monitoring—present status and applications, Sens. Actuators A: Phys. 147 (1) (2008) 150–164.
[27] J.R. Delmas, Optoelectronic Displacement Sensor US4338722 A, Microlec, S.A, 1982.
[28] M. Kaufmann, et al., Optoelectronic Displacement Sensor with Correction Filter, US4812635 A, BBC Brown Boveri, Ag, 1989.
[29] Y. Shan, J.E. Speich, K.K. Leang, Low-cost IR reflective sensors for submicrolevel position measurement and control, Mechatron. IEEE/ASME Trans. 13 (6) (2008) 700–709.
[30] G. Benet, et al., Using infrared sensors for distance measurement in mobile robots, Rob. Auton. Syst. 40 (4) (2002) 255–266.
[31] A. Potdar, et al., Development of modular machine tool structural monitoring system, in: Proceedings of the International Conference on Advanced Manufacturing Engineering and Technologies, KTH Royal Institute of Technology, Stockholm, 2013.
[32] ISO, 5725-1 Accuracy (Trueness and Precision) of Measurement Methods and Results, International Standards Organization, 1994.

## Biographies

**Akshay Potdar**, has completed his B. Eng. in electronics and tele-communication engineering from Mumbai University, India and M.Sc (distinction) in engineering control systems and instrumentation from University of Huddersfield, UK. He has industrial experience in process instrumentation and automation. He is presently working in the field of on-machine probing and sensor fusion and is PhD candidate at Centre for Precision Technologies at University of Huddersfield, UK.

**Dr. Andrew P. Longstaff**, has an honours degree in mathematics and a PhD in, "Methods of evaluation of the positioning capability of Cartesian and non-Cartesian machines," under the supervision of Professor Derek Ford at the University of Huddersfield. He is active in the area of industrial metrology and automation. He has worked on several successful UK Engineering and Physical Science Research Council (EPSRC) and EU-government funded projects involving the development and evaluation of new sensors and measurement devices.

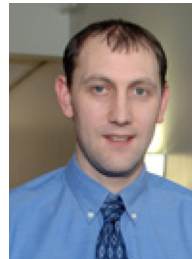

**Dr. Simon Fletcher**, is a Principal Enterprise Fellow in the Engineering Control and Machine Performance Group (ECMPG) at the University of Huddersfield. After gaining an honours degree in Computer Aided Engineering, he joined the group and began research into machine tool performance and completed his PhD in 'Computer aided system for intelligent implementation of machine tool error reduction strategies'. Dr. Fletcher has been directly involved at various levels in nearly all the projects successfully undertaken by the group including the EPSRC Centre of Innovative Manufacture in Advanced Metrology and various European, UK government and industry projects. He is active in the area of machine tool simulation and advanced metrology.